# 10

# Case Study: Taylor–Sedov Blast Wave

## 10.1 BRIEF BACKGROUND TO THE PROBLEM

Back in 1945 Sir Geoffrey Ingram Taylor was asked by the British MAUD (Military Application of Uranium Detonation) Committee to deduce information regarding the power of the first atomic explosion at the Trinity site in the New Mexico desert. He derived some remarkable results, which were based on his earlier classified work [Tay-41], and was able to estimate, using only public domain photographs of the blast, that the yield of the bomb was equivalent to between 16.8 and 23.7 kilotons of TNT, depending upon which value for the isentropic exponent for air was assumed. Each of these photographs, declassified in 1947, crucially, contained a distance scale and precise time (see, e.g., Figs. 10.1 and 10.3). Ingram's calculation was classified secret but, five years later he published the details [Tay-50a, Tay-50b], much to the consternation of the British government. John von Neumann and Leonid Ivanovitch Sedov published similar independently derived results [Bet-47, Sed-46]. Later Sedov also published a full analytical analysis [Sed-59] (see Appendix 10.B at the end of this chapter). For further interesting discussion relating to the theory, refer to [Deb-58, Kam-00, Pet-08].

The *Manhattan project* , also known as the *Trinity project*, was the code name for the secret U.S. project set up in 1942 to develop an atomic bomb.

## 10.2 SYSTEM ANALYSIS

The Taylor–Sedov blast is generally defined to be a spherical explosion caused by the point injection of energy. In general physics this energy could derive from the detonation of an explosive device and in astrophysics it could derive from a supernova. Here, we are primarily concerned with the detonation of a powerful explosive device.

Taylor analyzed the blast wave using the equivalent of the following equations:

$$\begin{aligned} \frac{\partial \rho}{\partial t} + \frac{\partial \rho u}{\partial r} + (\nu - 1)\frac{\rho u}{r} &= 0, \\ \frac{\partial u}{\partial t} + u\frac{\partial u}{\partial r} + \frac{1}{\rho}\frac{\partial p}{\partial r} &= 0, \\ \frac{\partial (p/\rho^{\gamma})}{\partial t} + u\frac{\partial (p/\rho^{\gamma})}{\partial r} &= 0, \end{aligned} \tag{10.1}$$

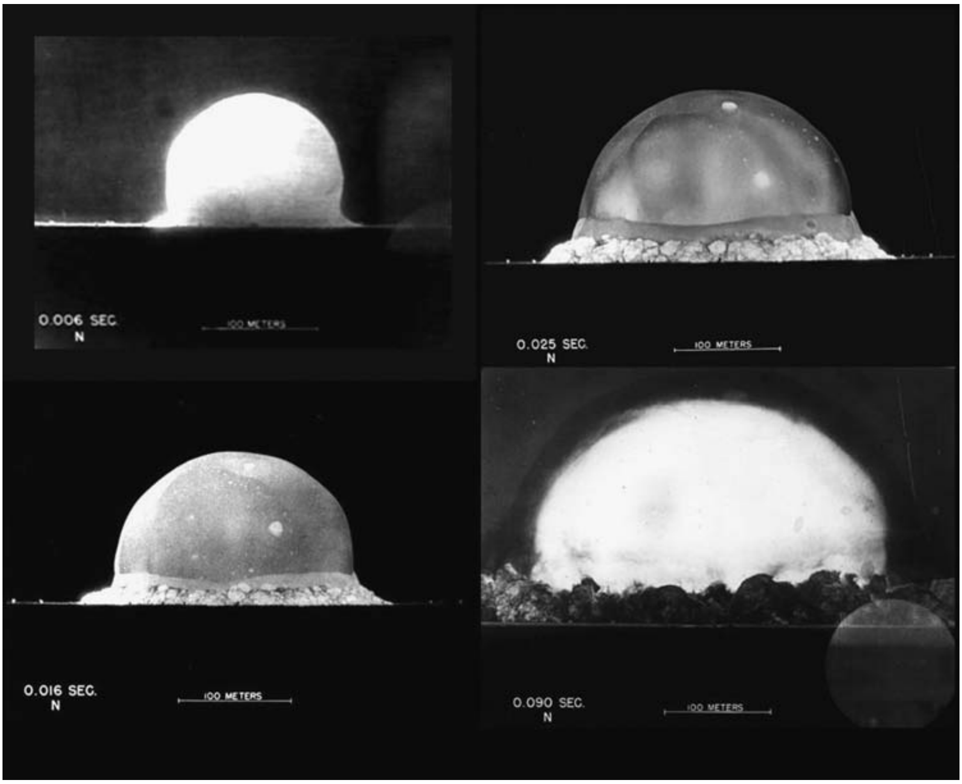


**Figure 10.1.** Time-lapse photographs with distance scales (100 m) of the first atomic bomb explosion in the New Mexico desert at 5:29 a.m. on July 16, 1945 [Mac-49]. Times from instant of detonation are indicated in bottom left corner of each photograph. See also Fig. 10.3.

where $t$ represents *time* and $\rho$, $u$, $p$, $r$, and $\gamma$ represent *density*, *velocity*, *pressure*, *radial coordinate*, and *isentropic exponent* (ratio of specific heats) of the medium, respectively. In addition, $\nu$ is a constant dependent upon the geometry of the problem: $\nu = 1$ for *planar flow*, $\nu = 2$ for *cylindrical symmetry*, and $\nu = 3$ for *spherical symmetry*. Also, like Taylor, we will be dealing with spherical symmetry where gravitation effects are ignored.

The effect of the explosion is to force most of the air within the shock wave into a thin shell just inside blast front. As the front expands, the maximum pressure decreases until, at about 10 atm, the analysis ceases to be accurate.

Now, if we assume we are dealing with an ideal problem such that

- the blast can be considered to result from a point source of energy
- the process is *isentropic* and the medium can be represented by the *equation of state* $(\gamma - 1)\, e = p/\rho$, where $e$ represents *internal energy per unit mass*
- there is spherical symmetry

then, similarity considerations (see Appendix 10.A at the end of this chapter) lead to the following equation [Tay-50b]:

$$R = S(\gamma)t^{2/5}E^{1/5}\rho_0^{-1/5}, \tag{10.2}$$

where, for a consistent set of units, $S(\gamma)$ is a *constant* that depends solely on $\gamma$, $R$ is the *radius of the wave front*, $\rho_0$ is initial density of the medium, and $E$ is the *total energy* released by the explosion. Equation (10.2) together with the *gas laws* enables a solution to eqns. (10.1) to be found.

Sir Geoffrey Ingram solved the PDEs (10.1) by first transforming them to a set of ordinary differential equations (ODEs), and, then applying numerical integration. By this method he arrived at a value of $K = 0.856 = S^{-5}$ [Tay-50b, Table 3], for an explosion in air, which compares well with the analytical value of $K = 0.851$ derived subsequently by Sedov via a lengthy complex calculation [Sed-59, p231]. The fact that Taylor could obtain such a close value is remarkable considering the lengthy serial calculations involved and that he would have had to use pencil and paper techniques, for example, *log tables*. Computer calculations using modern numerical integrators show that Taylor's method converges to the correct analytical value (discussed subsequently).

Following the general approach and nomenclature of Taylor [Tay-50a], we adopt the same similarity assumptions[1] for an expanding, spherically symmetric blast wave of constant total energy:

$$\begin{aligned} \text{Pressure:}\quad & p/p_0 = y = R^{-3} f_1, \\ \text{Density:}\quad & \rho/\rho_0 = \psi, \\ \text{Radial Velocity:}\quad & u = R^{-\frac{3}{2}}\phi_1, \end{aligned} \tag{10.3}$$

where $R$ is the radius of the shock wave forming the outer edge of the disturbance, with $p_0$ and $\rho_0$ being the pressure and density of the undisturbed atmosphere. If we define $r$ as being the radial co-ordinate, then $\eta = r/R$ and $f_1, \phi_1$, and $\psi$ are functions of $\eta$. It will be shown that these assumptions are consistent with the equations of motion and also with the equation of state of a perfect gas.

Substituting eqns. (10.3) into the second of eqns. (10.1), the *momentum equation*, we obtain

$$-\left(\frac{3}{2}\phi_1 + \eta\phi_1'\right) R^{-\frac{5}{2}} \frac{dR}{dt} + R^{-4}\left(\phi_1\phi_1' + \frac{p_0}{\rho_0}\frac{f_1'}{\psi}\right) = 0, \tag{10.4}$$

where we use a *prime* to denote differentiation with respect to $\eta$.

Now it is clear that for eqn. (10.4) to be correct and consistent with eqn. (10.2), it follows that we must have

$$\frac{dR}{dt} = AR^{-\frac{3}{2}}, \tag{10.5}$$

where

$$A = 2\frac{\phi_1\phi_1'\rho_0\psi + p_0 f_1'}{\rho_0\psi(2\phi_1'\eta + 3\phi_1)} = \text{constant}. \tag{10.6}$$

This is because $p_0$ and $p_0$ are constants and $\phi$, $\psi$, and $f$ are only functions of $\eta$. Thus, if $A$ was not a constant, then the blast speed $dR/dt$ would be a function of $\eta$ which is not physically realistic. The value $A = 3.267 \times 10^{11}$ is derived in what follows, where it is assumed that the units for $R$ and $t$ are centimeters and seconds respectively (see eqn. (10.49)).

[1] These assumptions facilitate the calculations that follow and demonstrate Taylor's deep understanding of the problem. They are not unique, and Sedov uses a slightly different set [Sed-59, p. 217].

Recall from the differential calculus that

$$\frac{\partial(\cdot)}{\partial t} = \frac{\partial(\cdot)}{\partial \eta}\frac{\partial \eta}{\partial R}\frac{\partial R}{\partial t}. \tag{10.7}$$

Substituting eqns. (10.3) and (10.5) into the first of eqns. (10.1), the *continuity equation*, and making use of eqn. (10.7), we obtain

$$-A\eta\psi' + \psi'\phi_1 + \psi\left(\phi_1' + \frac{2}{\eta}\phi_1\right) = 0. \tag{10.8}$$

Substituting eqns. (10.3) and (10.5) into the third of eqns. (10.1), the *equation of state*, and again making use of eqn. (10.7), we obtain

$$-A(3f_1 + \eta f_1') + \frac{\gamma f_1}{\psi}\psi'(-A\eta + \phi_1) - \phi_1 f_1' = 0. \tag{10.9}$$

We can now simplify the above equations by employing the following transformations

$$\begin{aligned} f &= f_1 a^2/A^2, \\ \phi &= \phi_1/A, \end{aligned} \tag{10.10}$$

where $a^2 = \gamma p_0/\rho_0$ is the velocity of sound in air, when we obtain

$$\begin{aligned} \phi'(\eta - \phi) &= \frac{1}{\gamma}\frac{f'}{\psi} - \frac{3}{2}\phi, \\ \frac{\psi'}{\psi} &= \frac{\phi' + 2\phi/\eta}{\eta - \phi}, \\ 3f + \eta f' + \frac{\gamma\psi'}{\psi}f(-\eta + \phi) - \phi f' &= 0. \end{aligned} \tag{10.11}$$

On solving for the primed variables in eqns. (10.11), we obtain the following three coupled ODEs:

$$\begin{aligned} f' &= \frac{6f\psi(-\eta + \phi)\eta + f\eta\phi\gamma\psi - 4f\phi^2\gamma\psi}{2\eta^3\psi - 4\eta^2\psi\phi - 2f\eta + 2\phi^2\psi\eta}, \\ \phi' &= \frac{1}{2}\frac{3\eta\gamma\psi\phi^2 - 3\phi\eta^2\gamma\psi + 4\phi f\gamma - 6f\eta}{\eta(\eta^2\psi - 2\eta\psi\phi - f + \phi^2\psi)\gamma}, \\ \psi' &= -\frac{1}{2}\frac{(4\gamma\psi\phi^3 - 5\eta\gamma\psi\phi^2 + \phi\eta^2\gamma\psi - 6f\eta)\psi}{\eta(\eta^2\psi - 2\eta\psi\phi - f + \phi^2\psi)\gamma(-\eta + \phi)}, \end{aligned} \tag{10.12}$$

which is a quite extraordinary result.

We have now reached a situation where we have transformed the problem represented by the three partial differential equations of eqn, (10.1) to a simpler problem represented by the three ordinary differential equations of eqn. (10.12). Thus, if values for $f$, $\phi$, and $\psi$ are known for a given value of $\eta$, then additional values for $f$, $\phi$, and $\psi$ can be obtained by means of numerical integration.

The preceding calculations are a testament to Taylor's ability and insight. However, they are tedious to perform by hand. So, as an extra resource that readers may find useful, we include with the downloads code written for symbolic algebra programs Maple and Maxima (open source) that derive eqns. (10.12) from Taylor's orginal PDEs.

## 10.3 SOME USEFUL GAS LAW RELATIONS

We assume that we are dealing with a gas that obeys the *ideal gas law*,

$$pv = \mathcal{R}T, \tag{10.13}$$

where $p$ represents *pressure*, $v = 1/\rho$ *specific volume*, $\rho$ *density*, $T$ *temperature*, and $\mathcal{R}$ the *gas constant*.

We define the following simple relationships:

$$\begin{aligned} de &= C_v dT, \\ dh &= C_p dT, \\ h &= e + p/\rho, \\ a^2 &= \gamma p/\rho = \gamma \mathcal{R}T, \end{aligned} \tag{10.14}$$

where $e$ represents *internal energy h enthalpy*, $C_v$ *specific heat at constant volume*, $C_p$ *specific heat at constant pressure*, *a speed of sound* in the gas, and $\gamma = C_p/C_v$ *ratio of specific heats*.

Additionally, we assume that $C_p$ and $C_v$ are constants and independent of temperature. Such a gas is called a *calorically perfect gas* and, under these conditions, the internal energy and enthalpy relationships of eqns. (10.14) become

$$\begin{aligned} e &= C_v T \\ h &= C_p T. \end{aligned} \tag{10.15}$$

The differential forms of eqn. (10.13) and $h$ are

$$\begin{aligned} p\,dv + v\,dp &= \mathcal{R}\,dT \\ dh &= de + p\,dv + v\,dp. \end{aligned} \tag{10.16}$$

Therefore, it follows from eqns. (10.14) and (10.16) that

$$\mathcal{R} = C_p - C_v. \tag{10.17}$$

The following represent the *Rankine–Hugonoit* conditions, which relate thermodynamic properties across a shock. They always hold for flow velocities under adiabatic conditions, regardless of whether the shock is stationary or moving:

$$\begin{aligned} &\text{Continuity:} && \rho_1 u_1 = \rho_0 u_0, \\ &\text{Momentum:} && p_1 + \rho_1 u_1^2 = p_0 + \rho_0 u_0^2, \\ &\text{Energy:} && \rho_1 u_1 \left(e_1 + \tfrac{1}{2}u_1^2 + p_1/\rho_1\right) = \rho_0 u_0 \left(e_0 + \tfrac{1}{2}u_0^2 + p_0/\rho_0\right). \end{aligned} \tag{10.18}$$

Subscripts 1 and 0 indicate conditions immediately upstream and downstream of the shock, respectively.

Now consider the situation shown in Fig. 10.2, where a moving piston introduces a shock wave into the system. The piston creates a shock that proceeds at a velocity greater than that of the piston itself. In this situation, the velocity immediately behind the shock wave is equal to $u_s - u_p$ and eqns. (10.18) become

$$\begin{aligned} &\text{Continuity:} && \rho_1(u_s - u_p) = \rho_0 u_s, \\ &\text{Momentum:} && p_1 + \rho_1(u_s - u_p)^2 = p_0 + \rho_0 u_s^2, \\ &\text{Energy:} && e_1 + \tfrac{1}{2}(u_s - u_p)^2 + p_1/\rho_1 = e_0 + \tfrac{1}{2}u_s^2 + p_0/\rho_0, \end{aligned} \tag{10.19}$$

where the continuity equation has been used to simplify the energy equation.

https://doi.org/10.1017/CBO9781316336069.011 Published online by Cambridge University Press

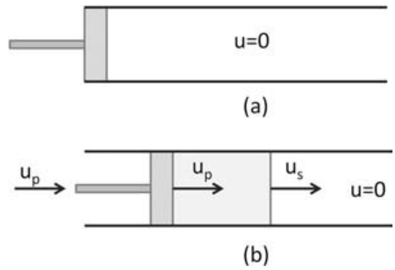


**Figure 10.2.** Shock tube containing a piston. (a) With piston stationary. (b) With piston moving at constant velocity, $u_p$, and the shock wave moving with velocity, $u_s$, into a stationary gas.

On substituting the continuity equation into the momentum equation and rearranging, we obtain

$$(u_s - u_p)^2 = \frac{p_0 - p_1}{\rho_0 - \rho_1}\left(\frac{\rho_0}{\rho_1}\right). \tag{10.20}$$

Substituting this result and the continuity equation into the energy equation yields

$$e_0 - e_1 = \frac{p_1 + p_0}{2}\left(\frac{1}{\rho_1} - \frac{1}{\rho_0}\right). \tag{10.21}$$

Eliminating internal energy by use of the equation of state, $(\gamma - 1)\, e = p/\rho$, and rearranging leads to the following important result [Tay-50a, eqn. (15)]:

$$\frac{\rho_1}{\rho_0} = \frac{1 + \dfrac{\gamma+1}{\gamma-1}\dfrac{p_1}{p_0}}{\dfrac{\gamma+1}{\gamma-1} + \dfrac{p_1}{p_0}}. \tag{10.22}$$

Alternatively, we can rearrange eqn. (10.21) by using the relationships $e = C_v T$ and $\rho = p/RT$ to obtain

$$\frac{T_1}{T_0} = \frac{p_1}{p_0}\left(\frac{\dfrac{\gamma+1}{\gamma-1} + \dfrac{p_1}{p_0}}{1 + \dfrac{\gamma+1}{\gamma-1}\dfrac{p_1}{p_0}}\right) = \frac{p_1}{p_0}\frac{\rho_0}{\rho_1}. \tag{10.23}$$

Rearranging the continuity equation of eqns. (10.19), we obtain

$$\frac{u_p}{u_s} = 1 - \frac{\rho_1}{\rho_0}, \tag{10.24}$$

which, on using eqn. (10.22), yields a second important result [Tay-50a, eqn. (17)]:

$$\frac{u_p}{u_s} = \frac{2\,(p_0/p_1 - 1)}{\gamma + 1 + (\gamma - 1)(p_0/p_1)}. \tag{10.25}$$

Now, a basic relationship that links the pressure ratio, $y_1 = p_1/p_0$, and the *Mach number*, $M_s = u_s/a_0$, is

$$\frac{p_1}{p_0} = 1 + \frac{2\gamma}{\gamma+1}\left(M_s^2 - 1\right), \tag{10.26}$$

which, on rearranging, yields a third important result [Tay-50a, eqn. (16)]:

$$\frac{u_s^2}{a_0^2} = \frac{1}{2\gamma}\left\{\gamma - 1 + (\gamma+1)\frac{p_1}{p_0}\right\}. \tag{10.27}$$

The important results derived here facilitate solution of the blast wave eqns. (10.1).

The downloads include code written for symbolic algebra programs Maple and Maxima (open source) that derive eqns. (10.22), (10.25), and (10.27) from the Rankine–Hugonoit conditions.

## 10.4 SHOCK WAVE CONDITIONS

The following equations were derived earlier from the Rankine–Hugonoit eqns. (10.19):

$$\begin{aligned}
\frac{\rho_1}{\rho_0} &= \frac{(\gamma-1)+(\gamma+1)y_1}{(\gamma+1)+(\gamma-1)y_1},\\
\frac{U^2}{a^2} &= \frac{1}{2\gamma}\{\gamma-1+(\gamma+1)y_1\},\\
\frac{u_1}{U} &= \frac{2(y_1-1)}{\gamma-1+(\gamma+1)y_1},
\end{aligned} \tag{10.28}$$

where $\rho_1, u_1$, and $y_1$ represent values of $\rho, u$, and $p$, respectively, immediately behind the shock wave and $U = dR/dt$ ($U = u_s$ and $u_1 = u_p$ in Section 10.3) is the radial velocity of the shock wave. Ambient conditions are indicated by the subscript 0.

It follows from eqns. (10.28) that the *strong shock* conditions, where $y_1 = p_1/p_0 \gg 1$ at the shock boundary, are

$$\begin{aligned}
\frac{\rho_1}{\rho_0} &= \frac{\gamma+1}{\gamma-1},\\
\frac{U^2}{a^2} &= \frac{\gamma+1}{2\gamma}y_1,\\
\frac{u_1}{U} &= \frac{2}{\gamma+1},
\end{aligned} \tag{10.29}$$

Note that the second of eqns. (10.29) is a corrected version of Taylor's eqn. (16a) [Tay-50a].

Now, from eqns. (10.3), (10.5), and (10.10), we have

$$\begin{aligned}
\psi &= \rho_1/\rho_0,\\
\phi &= \phi_1/A = u_1 R^{3/2}/A = u_1/U,\\
f &= f_1 a^2/A^2 = y_1 a^2 R^3/A^2 = y_1 a^2/U^2 = 2\gamma/(\gamma+1).
\end{aligned} \tag{10.30}$$

Thus, it follows that at the shock boundary, that is, at $\eta = 1$, we have

$$\begin{aligned}
\psi(1) &= \frac{\gamma+1}{\gamma-1},\\
f(1) &= \frac{2\gamma}{\gamma+1},\\
\phi(1) &= \frac{2}{\gamma+1}.
\end{aligned} \tag{10.31}$$

These values can be used as the starting point to obtain a (step by step) solution to eqns. (10.12) by means of numerical integration.

## 10.5 ENERGY

The total energy $E$ of the disturbance may be regarded as consisting of two parts, the kinetic energy

$$K.E. = 4\pi \int_0^R \frac{1}{2}\rho u^2 r^2 dr \tag{10.32}$$

and the heat energy

$$H.E. = 4\pi \int_0^R \frac{pr^2}{\gamma - 1} dr. \tag{10.33}$$

In terms of the variables $f, \phi, \psi$, and $\eta$, we have

$$E = K.E. + H.E. = 4\pi A^2 \left\{ \frac{1}{2}\rho_0 \int_0^1 \psi\phi^2\eta^2 d\eta + \frac{p_0}{a_0^2(\gamma - 1)} \int_0^1 f\eta^2 d\eta \right\}, \tag{10.34}$$

or, alternatively, because $p_0 = a_0^2\rho_0/\gamma$,

$$E = B\rho_0 A^2, \tag{10.35}$$

where $B$ is a function of $\gamma$ only, and whose value is

$$B = 2\pi \int_0^1 \psi\phi^2\eta^2 d\eta + \frac{4\pi}{\gamma(\gamma - 1)} \int_0^1 f\eta^2 d\eta. \tag{10.36}$$

Because the integrals in (10.36) are both functions of $\gamma$ only, it appears that for a given value of $\gamma$, $A^2$ is simply proportional to $E/\rho_0$.

Equating eqn. (10.5) and (10.70) from Appendix 10.A at the end of this chapter yields

$$A = \frac{2}{5} R^{\frac{5}{2}} t^{-1}. \tag{10.37}$$

Recall from eqn. (10.2) that

$$R = S(\gamma) t^{2/5} E^{1/5} \rho_0^{-1/5}. \tag{10.38}$$

It therefore follows from eqns. (10.35) and (10.37) that

$$S(\gamma) = \left( \frac{25}{4B} \right)^{1/5}. \tag{10.39}$$

Thus, once $B$ is found by numerical integration, $S(\gamma)$ is known and, hence, the total energy of the explosion can be calculated. Taylor actually derives the variable $K = S^{-5}$ [Tay-50b, eqn. (8)]. Note that the constant $S(\gamma)$ in eqn. (10.39) is the same $S$ as derived in eqn. (10.67) and that $K$ is equal to the constant $\alpha$ used by Sedov [Sed-59, p. 213].

https://doi.org/10.1017/CBO9781316336069.011 Published online by Cambridge University Press

## 10.6 PHOTOGRAPHIC EVIDENCE

The photograph strips shown in Fig. 10.3 provided Taylor with crucial evidence upon which he could finally narrow down the physical solution of the Trinity blast wave problem. By carefully measuring the width of the blast wave for each photograph and plotting these values against the corresponding time it was taken following the blast, the relationship between blast radius $R$ and elapsed time $t$, was determined. The figures published by Taylor are shown in Table 10.1 and have also been plotted in Fig. 10.4. These data enabled Taylor to determine the constant in eqn. (10.69) and establish the following relationship between $R$ and $t$:

$$\frac{5}{2}\log_{10} R - \log_{10} t = 11.915. \tag{10.40}$$

Equation (10.40) is equivalent to

$$R^5 t^{-2} = 6.67 \times 10^{23}, \tag{10.41}$$

where the units for $R$ are centimeters and the units for $t$ are seconds.

**Table 10.1.** Radius $R$ of blast wave at time $t$ after the explosion. The data are based on Table 1 from [Tay-50b], which tabulated measurements from high-speed photographs that were taken of the Trinity explosion. The units for time in column 1 are milliseconds, and for column 3 they are seconds. The units for $R$ in column 2 are meters and in columns 4 and 5 they are centimeters

| $t$ | R | $\log_{10}(t)$ | $\log_{10}(R)$ | $\frac{5}{2}\log_{10}(R)$ |
|---|---|---|---|---|
| 0.1 | 11.1 | $\bar{4}.0$ | 3.045 | 7.613 |
| 0.24 | 19.9 | $\bar{4}.38$ | 3.298 | 8.244 |
| 0.38 | 25.4 | $\bar{4}.58$ | 3.405 | 8.512 |
| 0.52 | 28.8 | $\bar{4}.716$ | 3.458 | 8.646 |
| 0.66 | 31.9 | $\bar{4}.82$ | 3.504 | 8.759 |
| 0.8 | 34.2 | $\bar{4}.903$ | 3.535 | 8.836 |
| 0.94 | 36.3 | $\bar{4}.973$ | 3.56 | 8.901 |
| 1.08 | 38.9 | $\bar{3}.033$ | 3.59 | 8.976 |
| 1.22 | 41.0 | $\bar{3}.086$ | 3.613 | 9.032 |
| 1.36 | 42.8 | $\bar{3}.134$ | 3.631 | 9.079 |
| 1.5 | 44.4 | $\bar{3}.176$ | 3.647 | 9.119 |
| 1.65 | 46.0 | $\bar{3}.217$ | 3.663 | 9.157 |
| 1.79 | 46.9 | $\bar{3}.257$ | 3.672 | 9.179 |
| 1.93 | 48.7 | $\bar{3}.286$ | 3.688 | 9.22 |
| 3.26 | 59.0 | $\bar{3}.513$ | 3.771 | 9.427 |
| 3.53 | 61.1 | $\bar{3}.548$ | 3.786 | 9.466 |
| 3.8 | 62.9 | $\bar{3}.58$ | 3.798 | 9.496 |
| 4.07 | 64.3 | $\bar{3}.61$ | 3.809 | 9.521 |
| 4.34 | 65.6 | $\bar{3}.637$ | 3.817 | 9.543 |
| 4.61 | 67.3 | $\bar{3}.688$ | 3.828 | 9.57 |
| 15.0 | 106.5 | $\bar{2}.176$ | 4.027 | 10.068 |
| 25.0 | 130.0 | $\bar{2}.398$ | 4.114 | 10.285 |
| 34.0 | 145.0 | $\bar{2}.531$ | 4.161 | 10.403 |
| 53.0 | 175.0 | $\bar{2}.724$ | 4.243 | 10.607 |
| 62.0 | 185.0 | $\bar{2}.792$ | 4.267 | 10.668 |

https://doi.org/10.1017/CBO9781316336069.011 Published online by Cambridge University Press

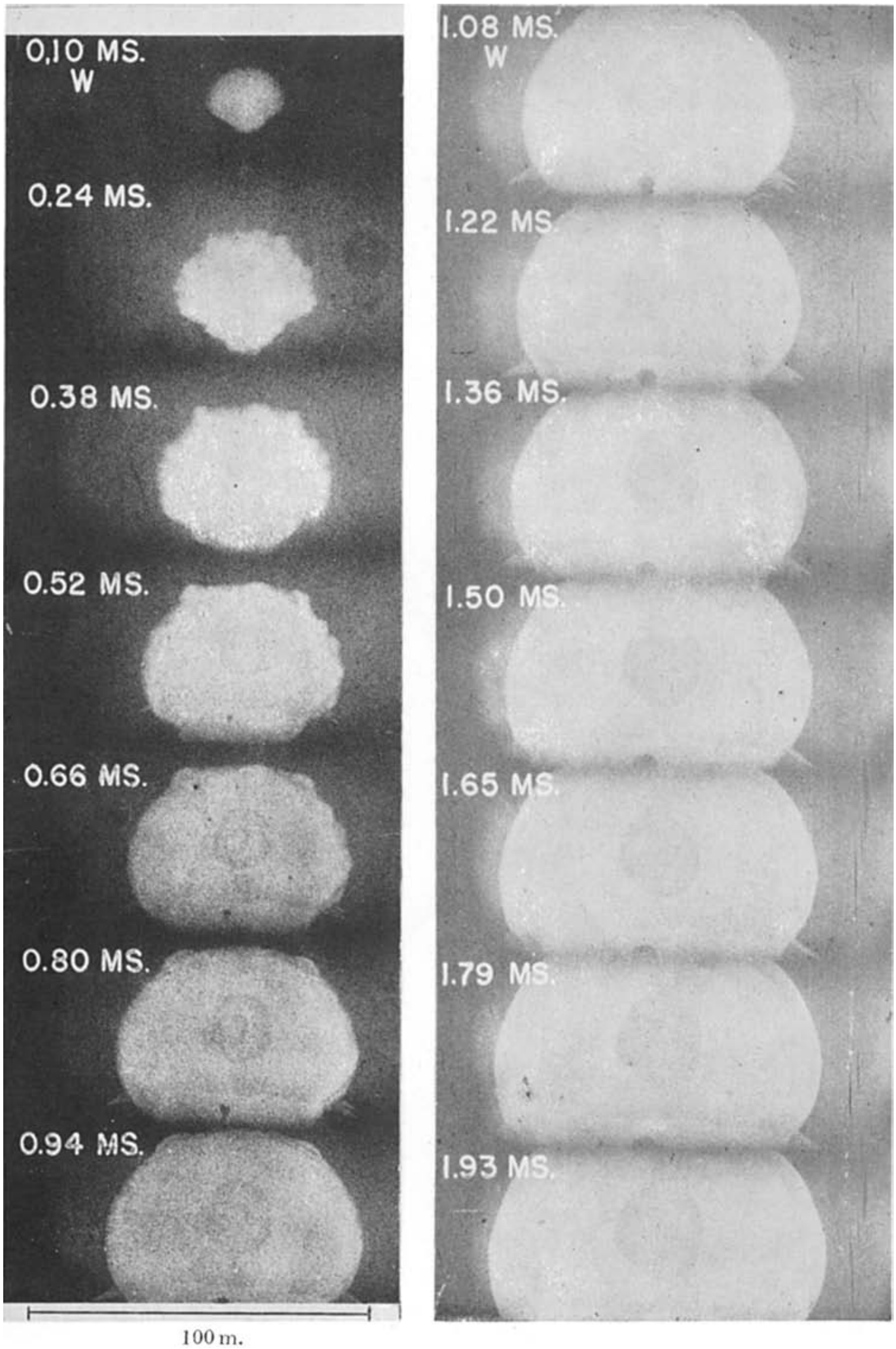


**Figure 10.3.** Photographic sequence of the Trinity atomic explosion with distance scale [Mac-49]. See also Fig. 10.1.

https://doi.org/10.1017/CBO9781316336069.011 Published online by Cambridge University Press

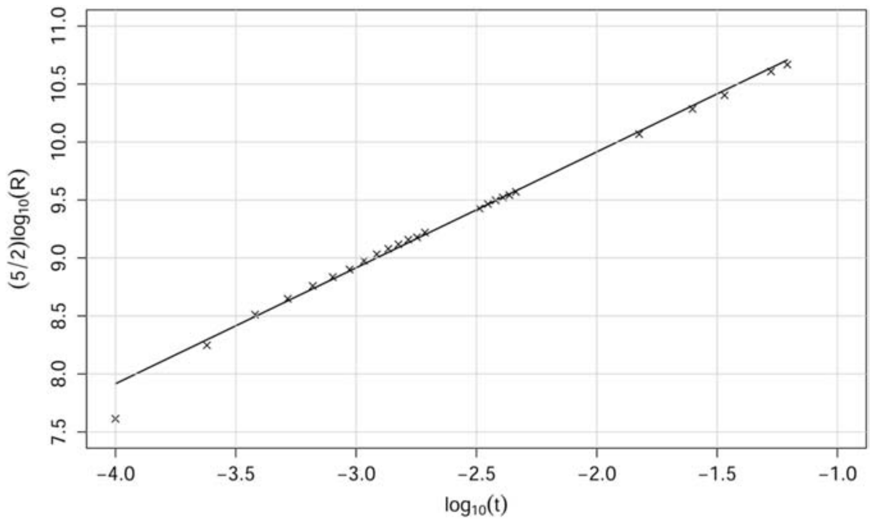


**Figure 10.4.** Data from Table 10.1 superimposed on a plot of the relation $\frac{5}{2}\log_{10} R - \log_{10} t = 11.915$. The units of $R$ are centimeters.

Thus, Taylor showed that the explosion fireball expanded very closely in accordance with the theoretical prediction [Tay-46] he made more than four years previously.

Note that the bar over the leading figure in the third column of Table 10.1 is how logarithms used to be presented for fractional numbers. To preserve precision, fractional quantities were shifted to the left until the leading figure immediately preceded the decimal point. Then this number was divided by a power of 10 to restore the number back to its correct value. For example, the number 0.00456 becomes 4.56/1000 and the logarithm was written as $\bar{3}.659$. This was understood to be equivalent to $-3 + 0.659$ or $-2.341$. This may seem cumbersome to the modern reader who has access to computers or calculators that are accurate to many significant figures. However, before these were available, hand calculations employed *logarithm* and *antilogarithm* tables with a limited number of significant figures (commonly five), and this method ensured that maximum precision was maintained.

The data for Table 10.1, in the form of a csv file, along with a R program to generate Fig. 10.4, have been included with the downloads for this book.

## 10.7 TRINITY SITE CONDITIONS

Operation TRINITY, conducted by the Manhattan Engineer District (MED), was designed to test and assess the effects of a nuclear weapon. The TRINITY device was detonated on a l00-foot tower at the Alamogordo Bombing Range in south central New Mexico at 5:30 A.M. on July 16, 1945. The yield of the detonation was equivalent to the energy released by detonating 21 kilotons of TNT. At shot time, the temperature was 21.8°C, and surface air pressure was 850 millibars. The winds were nearly calm at the surface; at 10,300 feet above mean sea level, they were from the southwest at 10 knots. The winds blew the cloud resulting from the detonation to the northeast. From July 1945

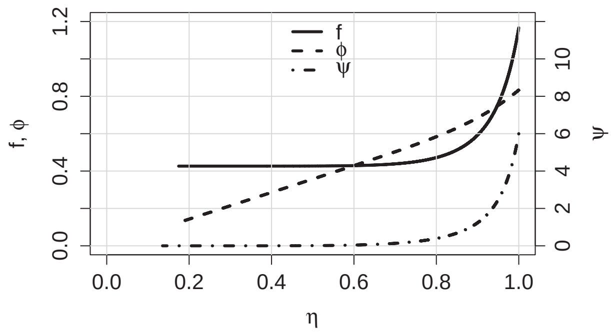


**Figure 10.5.** Plots of $f$, $\phi$, and $\psi$ resulting from numerical integration of eqns. (10.12).

through 1946, about 1,000 military and civilian personnel took part in Project TRINITY or visited the test site [Dtr-07].

## 10.8 NUMERICAL SOLUTION

Using the values given in eqns. (10.29) for $f$, $\phi$, and $\psi$ at the blast wave boundary, we are now in a position to integrate eqns. (10.12) numerically using the integrator `lsodes` from the package `deSolve`. The solutions are plotted in Fig. 10.5 using the ratio of specific heats for air, that is, $\gamma = 1.4$.

Now that $f$, $\phi$, and $\psi$ are known and so we can evaluate the integrals in eqn. (10.36), that is,

$$I_1 = \int_0^1 \psi \phi^2 \eta^2 d\eta \tag{10.42}$$

$$I_2 = \int_0^1 f \eta^2 d\eta. \tag{10.43}$$

However, we only have numerical values for $f$, $\phi$, and $\psi$, and therefore a quadrature method is required. We choose to employ the general-purpose *composite Simpson's rule*, that is,

$$\int_a^b f(x)\,dx \approx \frac{h}{3}\left[ f(x_0) + 2\sum_{j=1}^{n/2-1} f(x_{2j}) + 4\sum_{j=1}^{n/2} f(x_{2j-1}) + f(x_n) \right], \tag{10.44}$$

which has a fourth-order error equal to

$$-\frac{h^4}{180} h \max_{\xi \in [a,b]} |f^{(4)}(\xi)|. \tag{10.45}$$

The $\eta$-domain was represented by $N = 10{,}001$ points with an interval $h = (b - a)/(N - 1)$, and application of Simpson's rule resulted in the following values for $I_1$ and $I_2$:

$$I_1 = 0.1851699, \quad I_2 = 0.1851963. \tag{10.46}$$

The limits of integration were chosen as $a : \eta = 10^{-8}$ and $b : \eta = 1$. The lower limit can not be set exactly to *zero* as this causes the integral to become *singular*. However, this is not important as we can get sufficiently close to zero so that any error is insignificant. The value of $B$ can now be calculated as

$$B = 2\pi I_1 + \frac{4\pi}{\gamma(\gamma - 1)} I_2 = 5.319252, \tag{10.47}$$

which, in turn, enables $S$ and $K$ to be evaluated:

$$\begin{aligned} S &= \left(\tfrac{25}{4B}\right)^{1/5} = 1.0328 \\ K &= S^{-5} = 0.8510804. \end{aligned} \tag{10.48}$$

In addition the constant $A$ can be calculated from eqns. (10.37) and (10.41):

$$A = \frac{2}{5}\frac{R^{5/2}}{t} = 3.267 \times 10^{11}, \tag{10.49}$$

where the units of $R$ are centimeters.

The total energy of the blast can now be determined from eqn. (10.35) using $\rho_0 = 0.00125(\text{g/cm}^3)$ to give

$$\boxed{E_{tot} = B\rho_0 A^2 = 7.096 \times 10^{20}\ (\text{ergs}).\ [7.096 \times 10^4\ (\text{GJ})]} \tag{10.50}$$

The fact that the total energy of the blast can be predicted with good accuracy from, essentially, a set of time-lapsed photographs, is nothing less than a spectacular result.

Taylor defines the amount of energy liberated by one long ton[2] of TNT,[3] when exploded, to be $4.25 \times 10^{16}$ erg (4.25 GJ). Therefore, the amount of TNT, $M_{TNT}$, that the blast can be considered equivalent to is

$$M_{TNT} = E_{tot}/4.25 \times 10^{16} = 16{,}669\ (\text{ton}). \tag{10.51}$$

This is also referred to as the *yield* of the explosive device.

Values for $p$ and $T$ at any value of $\eta$ and $R$ can now be determined from eqns. (10.3), (10.10), (10.23), and (10.35) to give, for $\gamma = 1.4$,

$$\begin{aligned} p(\eta, R) &= p_0 R^{-3} f_1(\eta) = R^{-3} f(\eta)\frac{\rho_0 A^2}{\gamma} = R^{-3} f(\eta)\frac{E_{tot}}{B\gamma}, \\ \therefore p_s &= p(1, R) = 0.1343 R^{-3} f(1) E_{tot}, \end{aligned} \tag{10.52}$$

and

$$\begin{aligned} T(\eta, R) &= T_0 \frac{p(\eta, R)}{p_0}\frac{1}{\psi(\eta)}, \\ \therefore T_s &= T(1, R) = 0.1343 R^{-3} f(1) E_{tot} T_0/(p_0 \psi(1)). \end{aligned} \tag{10.53}$$

The shock pressure and temperature will occur at the blast wave position, which corresponds to $\eta = 1$, when $f(1) = 1.1667$ and $\psi(1) = 6$. Figure 10.6 shows a plot of $p_s$ and $T_s$ with respect to the distance from the center of the explosion, where $p_s$ has been divided by $10^6$ to convert from dynes/cm$^2$ to atm.

[2] One long ton is equal to 2240 lbs or 1016 kg.

[3] TNT is the acronym for the explosive substance *trinitrotoluene*. The explosive yield of TNT is considered to be the standard measure of strength of bombs and other explosives.

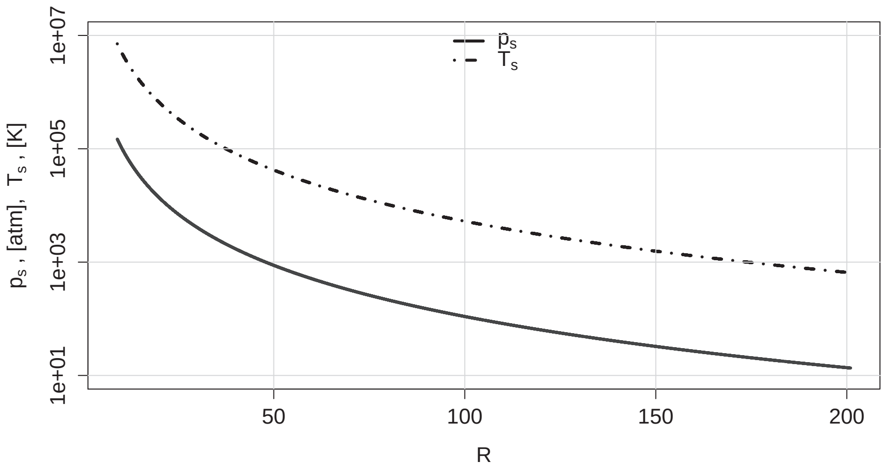


**Figure 10.6.** Plots of $p_{max}$ and $T_{max}$.

It also follows from eqns. (10.52) and (10.53) that

$$\frac{p(\eta)}{p_s} = \frac{p(\eta, R)}{p(1, R)} = \frac{f(\eta)}{f(1)} = \frac{1}{1.1667} f(\eta) \tag{10.54}$$

and

$$\frac{T(\eta)}{T_s} = \frac{T(\eta, R)}{T_(1, R)} = \frac{p(\eta)}{p(1)} \frac{\psi(1)}{\psi(\eta)} = 5.143 \frac{f(\eta)}{\psi(\eta)}. \tag{10.55}$$

Figure 10.7 shows a plot of $p(\eta)/p_s$ and $T(\eta)/T_s$ with respect to $\eta$. Note that there is no dependency on $R$ in eqns. (10.54) and (10.55), as the $R$ terms cancel.

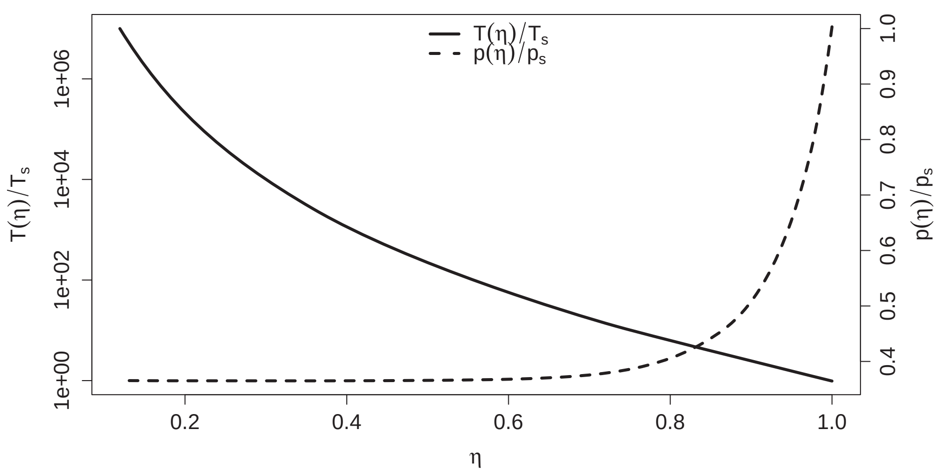


**Figure 10.7.** Plots of $p(\eta)/p_s$ and $T(\eta)/T_s$.

https://doi.org/10.1017/CBO9781316336069.011 Published online by Cambridge University Press

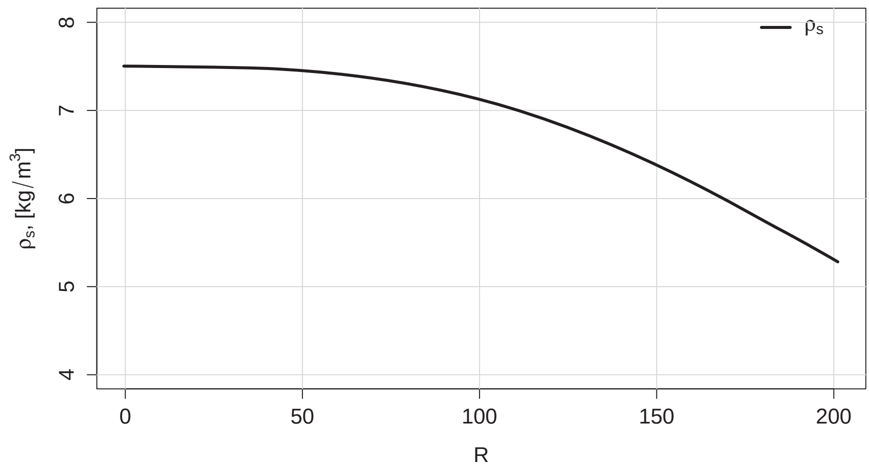


**Figure 10.8.** Plot of $\rho_s(\eta)$.

From eqn. (10.22) we see that

$$\rho_s = \rho(1, R) = \rho_0 \left( \frac{1 + \dfrac{\gamma+1}{\gamma-1}\dfrac{p_s}{p_0}}{\dfrac{\gamma+1}{\gamma-1} + \dfrac{p_s}{p_0}} \right). \tag{10.56}$$

Thus, using eqn. (10.52), we are able to plot $\rho_s$ as it evolves with the blast wave front (see Fig. 10.8). From eqns. (10.41) and (10.70) we see that the shock velocity is

$$u_s(t) = \frac{2}{5}\frac{R}{t} = \frac{2}{5}\left(\frac{6.67 \times 10^{23}}{t^3}\right)^{\frac{1}{5}}. \tag{10.57}$$

Therefore we can plot $u_s$ as it evolves with time. Similarly, from eqn. (10.38), we can plot the evolution of the blast front $R$ with time (see Fig. 10.9).

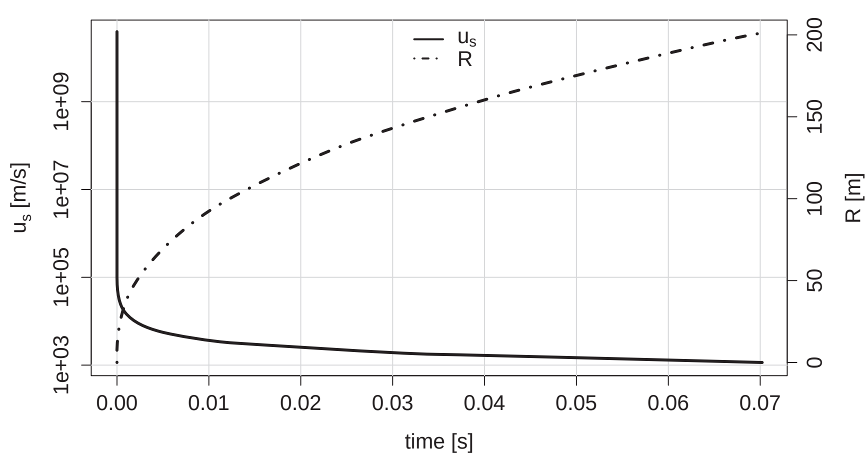


**Figure 10.9.** Plots of $u_s(t)$ and $R(t)$.

https://doi.org/10.1017/CBO9781316336069.011 Published online by Cambridge University Press

**Table 10.2.** Comparison of primary variable values from Taylor with those generated by computer

| Primary variable | Taylor result | Computer result |
|---|---|---|
| $I_1$ | 0.185 | 0.185 |
| $I_2$ | 0.187 | 0.185 |
| $K$ | 0.856 | 0.851 |
| $S$ | 1.0316 | 1.0328 |
| $E$ | $7.140 \times 10^{20}$ (erg) | $7.096 \times 10^{20}$ (erg) |
| $M_{TNT}$ | 16,800 (long-ton) | 16,696 (long-ton) |

*Note*: 1 erg = $10^{-7}$ J and 1 long ton = 2240 lbs/1016 kg.

From eqns. (10.3) and (10.10) we see that $u(\eta, R) = \phi(\eta)AR^{-3/2}$. But the shock velocity will occur at the blast wave position, which corresponds to $\eta = 1$. Therefore, it follows that

$$u(\eta)/u_s = u(\eta, R)/u(1, R) = \phi(\eta)/\phi(1), \tag{10.58}$$

where for $\gamma = 1.4$, we see from eqn. (10.31) that $\phi(1) = 2/2.4 = 0.833$.

We are now able to plot $u(\eta)/u_s$ against $\eta$ (see Fig. 10.10). Note that there is no dependency on $R$ in eqn. (10.58), as the $R$ terms cancel.

It is not certain exactly what numerical methods Taylor used in his step-by-step approach. However, he does indicate that steps of $\Delta\eta = 0.02$ were used together with a form of predictor corrector algorithm [Tay-50a, p. 163]. Nevertheless, whatever approach he did employ, it is clear that the method was extremely effective and produced very good results.

For comparison purposes, Table 10.2 lists Taylor's primary results alongside computer generated results obtained by the same method, but which employed a modern adaptive numerical integrator with the *absolute* and *relative errors* specified as $10^{-14}$.

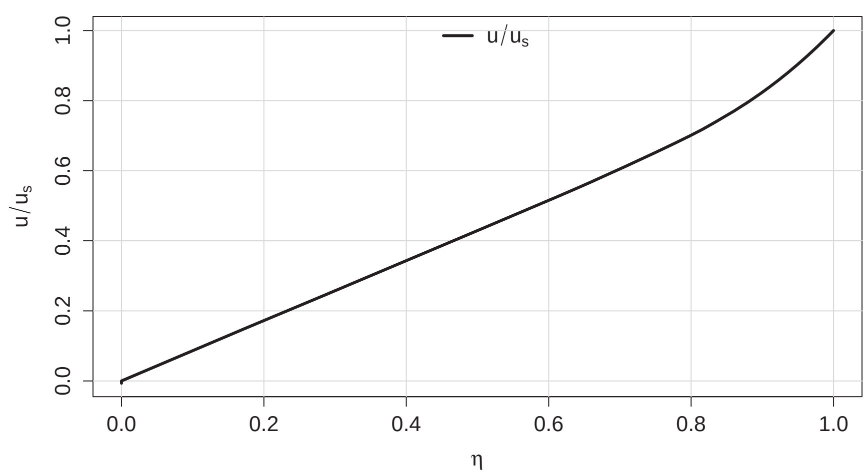


**Figure 10.10.** Plot of $u(\eta)/u_s$.

https://doi.org/10.1017/CBO9781316336069.011 Published online by Cambridge University Press

R programs that perform the preceding calculations are included in Listings 10.1–10.3.

```
# File: TaylorSedov_main.R
# ---------------------------------------------------------------------------
# Taylor-Sedov explosion example
# ---------------------------------------------------------------------------
#
rm(list = ls(all = TRUE)) # Delete workspace
#
# Load libraries
library("deSolve")
library("rgl")
#
# Load derivative function
source("TaylorSedov_deriv.R")
#
ptm = proc.time()
# Declare array sizes
N=100001; # Make an odd number for Simpson's Rule calc.
#
# Set parameters
h<-1/(N-1)
gamma <- 7/5
Rgas <- 287.058
# Site conditions
T0_site <- 21.8 +273 # [K], 21.8 [C]
p0_site <- 85000 # Pascals, 850000 dynes/cm2 (850mBar, 0.83888 Std Atmosphere)
rho0_site <- p0_site/(Rgas*T0_site) # kg/m3
# Initialize state variables - see book text
f0   <- 2*gamma/(gamma+1)
phi0 <- 2/(gamma+1)
psi0 <- (gamma+1)/(gamma-1)
etaf <- 1; eta0 <- 0.00000001
eta=seq(etaf, eta0, by=-1/N)
nout=length(eta)
#
# Initial condition
uini = c(f0,phi0,psi0)
#
# Initialze other variables
ncall=0
#
# ODE integration
parms<-c(N,gamma)
```

https://doi.org/10.1017/CBO9781316336069.011 Published online by Cambridge University Press

```
out<-lsodes(y=c(uini), times=eta, func=TaylorSedov_deriv, #verbose = TRUE,
            sparsetype = "sparseint", ynames = FALSE,
            rtol=1e-12,atol=1e-12,maxord=5,parms=parms)
# Extract solution data from integrator output
f   <- out[1:(N),2]
phi <- out[1:(N),3]
psi <- out[1:(N),4]
# Plot results
source("TaylorSedov_postSimCalcs.R")
cat(sprintf("\nCalculation time: %f\n",(proc.time()-ptm)[3]))
```

**Listing 10.1.** File: `TaylorSedov_main.R`—Code for *main* program that performs the numerical analysis of the Taylor–Sedov blast wave problem. It calls the derivative function `TaylorSedov_deriv()` and code to perform postsimulation calculations and generate plots given in Listings 10.2 and 10.3, respectively

```
# File: TaylorSedov_deriv.R
TaylorSedov_deriv = function(eta, u, parms) {
    #
    # Reshape vector u to f, phi and psi vectors
    f   <- u[1]
    phi <- u[2]
    psi <- u[3]
    #
    dfdeta  <- (6*f*psi*(-eta+phi)*eta+f*eta*phi*gamma*psi-4*f*phi^2*gamma*psi)/
               (2*eta^3*psi-4*eta^2*psi*phi-2*f*eta+2*phi^2*psi*eta)
    #
    dphideta <- (1/2)*(3*eta*gamma*psi*phi^2-3*phi*eta^2*gamma*psi+4*phi*f*gamma
        -6*f*eta)/
                    (eta*(eta^2*psi-2*eta*psi*phi-f+phi^2*psi)*gamma)
    #
    dpsideta <- -(1/2)*(4*gamma*psi*phi^3-5*eta*gamma*psi*phi^2+phi*eta^2*gamma
        *psi-6*f*eta)*psi/
                    (eta*(eta^2*psi-2*eta*psi*phi-f+phi^2*psi)*gamma*(-eta+phi))
    # Calculate time derivative
    dudeta = c(dfdeta,dphideta,dpsideta)
    #
    # update number of derivative calls
    ncall <<- ncall+1
    #
    # Return solution
    return(list(dudeta))
}
```

**Listing 10.2.** File: `TaylorSedov_deriv.R`—Code for derivative function `TaylorSedov_deriv()`, called from the main program of Listing 10.1

https://doi.org/10.1017/CBO9781316336069.011 Published online by Cambridge University Press

```
# File: TaylorSedov_postSimCalcs.R
#
# Energy integrals
dI1de <- psi*phi^2*eta^2
dI2de <- f*eta^2
#
# Integrate by Simpson's rule
I1 <- h*(1/3*(dI1de[1] + dI1de[N]) + 4/3*sum(dI1de[seq(2,(N-1),2)])
        + 2/3*sum(dI1de[seq(3,(N-2),2)]))
I2 <- h*(1/3*(dI2de[1] + dI2de[N]) + 4/3*sum(dI2de[seq(2,(N-1),2)])
        + 2/3*sum(dI2de[seq(3,(N-2),2)]))
#
B <- (2*pi*I1+(4*pi)/(gamma*(gamma-1))*I2)
S <- (25/(4*B))^{1/5}
K <- S^(-5)
c <- 1/K
#
TaylorData <- 1
###########################
# Set simulation conditions
if (TaylorData == 1) {
  # Taylor paper
  p_0 <- 1 #1.013250  #  [atm] (1013250 dynes/cm2) # CHECK !!!
  T_0 <- 288        #  [K] (15 [C])
  rho_0 <- 1.25e-3 #  [g/cm^3] {p178, Taylor II}
}else {
  # DTRA data for New mexico desert at time of blast
  p_0 <- p0_site/101325 # [atm]
  T_0 <- T0_site        # [K]
  rho_0 <- rho0_site/1000 # [g/cm3]
}
###########################
# Similarity Eqn
R5tm2 <- 6.67e23 # (R*100)^5/t^2 [cm^5/s^2]
E_tot <- K*rho_0*R5tm2 # ergs
E_TNT <- 4.25e16     # ergs
M_eqivTNT <- E_tot/E_TNT
R_max <- 201
R <- seq(1,N,1)*R_max/N
#R2 <- seq(1,R_max,8)
t <- sqrt(K*(R*100)^5*rho_0/E_tot)
us <- (2/5)*R/t # [m/s]
A <- (2/5)*(R[1]*100)^(5/2)/t[1] # = sqrt(E_tot/rho_0/B)
u_us <- phi/phi[1]
# Max pressure at any point from explosion
ps <- (1/(B*gamma))*E_tot*f[1]/(R*100)^3/(p_0*1013250) # Atm=(dynes/cm2)/1013250
```

```
# p_max2 <- 0.155*E_tot/(R*100)^3/10^6 eqn(35), Taylor Part 1
#
eta2 <- seq(eta0, etaf, by=1/(R_max))
Ts <- T_0*ps/p_0/psi[1] # [K]
#Ts_T0 <- (ps/p_0)^(1/gamma)/psi[1]
T_Ts <- (f/f[1])*(psi[1]/psi)
#
p_ps <- f/f[1]
#
rhos <- 1000*rho_0*(1+(ps/p_0)*(gamma+1)/(gamma-1))/
  ((gamma+1)/(gamma-1)+ps/p_0) # [kg/m3]
#
# rho_max <- rho_0*((gamma+1)/(gamma-1)+p_0/p_max)/(1+(p_0/p_max)*(gamma+1)/
    (gamma-1))
rho_rhos <- psi/psi[1]
#
# psi_max=psi[1]=max{rho/rho_0}=6; {Eqn(9), Taylor, Part II}
#############################
# Plot f, phi and psi againts eta
# Set margin to allow for multiple axes
par(mar = c(5,5,2,5))
plot(eta, f, ylab = expression(paste(f,", ",phi)),
     xlab=expression(eta), ylim=c(0,1.2),type="l",
     col="black", lty=1, lwd=3)
grid(nx = NULL, ny = NULL, col="lightgray", lwd = 1, lty=1)
#
lines(eta, phi, ylim=c(0,max(f)), xlab="", ylab="",
      type="l",lty=2,col="black", main="",
      xlim=c(etaf,eta0),lwd=3)
#
par(new = T)
plot(eta, psi, ylim=c(0,12),type="l", lwd=3,
     lty=4, col = "black",
     axes = F, xlab = NA, ylab = NA)
axis(side = 4)
mtext(text=expression(psi), side = 4, line = 3 )
#
legend("top",legend=c(expression(f),expression(phi),expression(psi)),
       lwd=c(3,3,3),lty=c(1,2,4),bty="n", col=c("black","black","black"))
#
# Plot V_blast and R againts time
# Set margin to allow for multiple axes
par(mar = c(5,5,2,5))
plot(t, us, log="y", ylab = expression(paste(u[s], " , [m/s]")),
     xlab="time , [s]", type="l",
     lty=1, lwd=3)
```

https://doi.org/10.1017/CBO9781316336069.011 Published online by Cambridge University Press

```
grid(nx = NULL, ny = NULL, col="lightgray", lwd = 1, lty=1)
#
par(new = T)
plot(t, R, type="l", lwd=3,
     lty=4, col = "black",
     axes = F, xlab = NA, ylab = NA)
axis(side = 4)
mtext(text="R , [m]", side = 4, line = 3 )
#
legend("top",legend=c(expression(paste(u[s])) , "R"),
       lwd=c(2,2),lty=c(1,4),bty="n", col=c("black","black"))
#####################
N2<-round(0.88*N) # reduced eta domain - central area not acurate
par(mar = c(5,5,2,5))
plot(eta[1:N2], T_Ts[1:N2],
     ylab = expression(paste(T(eta)/T[s])),
     xlab=expression(eta), log="y", ylim=c(1,10^7)
     ,type="l", col="black", lty=1, lwd=3)
#
par(new = T)
plot(eta[1:N2], p_ps[1:N2], ,type="l",
     lwd=3, lty=2, col = "black",
     axes = F, xlab = NA, ylab = NA)
axis(side = 4)
mtext(text=expression(paste(p(eta)/p[s])),
      side = 4, line = 3 )
legend("top",lwd=c(3,3),lty=c(1,2),bty="n",
       legend=c(expression(paste(T(eta)/T[s], " ")),
                expression(paste(p(eta)/p[s], " "))),
       col=c("black","black"))
#####################
# Plot p_max and T againts R
# Set margin to allow for multiple axes
par(mar = c(5,5,2,5))
plot(R[4500:N], ps[4500:N],
     ylab = expression(paste(p[s], " , [atm], ", T[s], " , [K]")),
     xlab=expression(R), log="y", ylim=c(10,10^7)
     ,type="l", col="black", lty=1, lwd=3)
#
lines(R[4500:N], Ts[4500:N], xlab="", ylab="",
      type="l",lty=2,col="black", main="",
      xlim=c(0,R_max),lwd=3)
#
legend("top",lwd=c(3,3),lty=c(1,2),bty="n",
       legend=c(expression(paste(p[s], " ")),
                expression(paste(T[s], " "))),
```

```
      col=c("black","black"))
grid(nx = NULL, ny = NULL, col="lightgray", lwd = 1, lty=1)
#
#######################
plot(R, rhos, ylim=c(4,8),type="l",
     lwd=3, lty=1, col = "black",
     xlab = expression(paste(R)),
     ylab = expression(paste(rho[s], ", [", kg/m^3,"]")))
legend("topright",lwd=c(3),lty=1,bty="n",
      legend=expression(paste(rho[s], "        ")),
      col=c("black"))
grid(nx = NULL, ny = NULL, col="lightgray", lwd = 1, lty=1)
#######################
plot(eta, u_us, type="l",
     lwd=3, lty=1, col = "black",
     xlab = expression(paste(eta)),
     ylab = expression(paste(u/u[s])))
legend("top",lwd=c(3),lty=1,bty="n",
      legend=expression(paste(u/u[s])),
      col=c("black"))
grid(nx = NULL, ny = NULL, col="lightgray", lwd = 1, lty=1)
########################
```

**Listing 10.3.** File: `TaylorSedov_postSimCalcs.R`—Code to perform post simulation calculations and generate plots, called from the main program of Listing 10.1

## 10.9 INTEGRATION OF PDES

As an alternative to eqns. (10.1), we can choose to solve a set of *conservative equations* with *source terms*, that is, in the form

$$\frac{\partial \mathbf{U}}{\partial t} + \frac{\partial \mathbf{F}(\mathbf{U})}{\partial r} = -\mathbf{S}(\mathbf{U}), \tag{10.59}$$

where $\mathbf{U}$ represents the state variable vector, $\mathbf{F}$ the flux vector, $r$ the radial direction, and $\mathbf{S}$ vector of source terms.

We define the problem in terms of the following *Euler equations* with $\mathbf{U} = [\rho, \rho u, E]^T$, $\mathbf{F} = [\rho u, \rho u^2 + p, (E+p)u]^T$, and $\mathbf{S} = \frac{(\nu-1)}{r}[\rho u, \rho u^2, (E+p)u]^T$:

$$\begin{aligned}
\frac{\partial \rho}{\partial t} + \frac{\partial \rho u}{\partial r} \qquad &= -\frac{(\nu-1)}{r}\rho u, \\
\frac{\partial \rho u}{\partial t} + \frac{\partial(\rho u^2 + p)}{\partial r} &= -\frac{(\nu-1)}{r}\rho u^2, \\
\frac{\partial E}{\partial t} + \frac{\partial\left((E+p)u\right)}{\partial r} &= -\frac{(\nu-1)}{r}\left(E+p\right)u,
\end{aligned} \tag{10.60}$$

where, again, $\nu = 1$ for the planar case, $\nu = 2$ for the cylindrical case, and $\nu = 3$ for the spherically symmetric case. The variables are as previously defined, with $E = \rho(e + \frac{1}{2}u^2)$ representing *total energy*. Equations (10.60) are presented in *conservative form with*

https://doi.org/10.1017/CBO9781316336069.011 Published online by Cambridge University Press

*source* as this facilitates solution by the finite volume method. Some 1D numerical solution examples are included in Chapter 6.

## 10.A APPENDIX: SIMILARITY ANALYSIS

*Similarity analysis*, also known as *dimensional analysis*, indicates that the fireball expands at a rate that depends upon the follow relevant physical variables: explosion energy $E_0$, ambient density $\rho_0$, instantaneous blast wave radius $R$, and time $t$. We employ the ansatz that these can be combined into an algebraic function, $f$, to form a dimensionless constant $c$, that is, $c = f(R, E_0, \rho_0, t)$.

Now, for a geometry-dependent system, the dimensions of each variable are

$$E_0 = [ML^{\nu-1}T^{-2}], \rho_0 = [ML^{-3}], R = [L], t = [T],$$

where $\nu$ is a constant dependent upon the geometry of the problem: $\nu = 1$ for *planar flow*, $\nu = 2$ for *cylindrical symmetry*, and $\nu = 3$ for *spherical symmetry*. On the basis of these assumptions, $R$ can be represented, dimensionally, by

$$[R] = [E_0]^x[\rho_0]^y[t]^z. \tag{10.61}$$

If we substitute in the appropriate dimensions for each variable, we obtain

$$[L] = [ML^{\nu-1}T^{-2}]^x[ML^{-3}]^y[T]^z. \tag{10.62}$$

Then, on expanding exponents, we obtain the following set of linear equations:

$$[L^1] = [M^{x+y}L^{(\nu-1)x-3y}T^{z-2x}]. \tag{10.63}$$

But the variable exponents for $L$, $M$, and $T$ must be equal on both sides of eqn. (10.63). This yields the following set of linear equations:

$$\begin{aligned} 1 &= (\nu-1)x \; -3y, \\ 0 &= \qquad\quad x \; +y, \\ 0 &= \qquad -2x \; +z, \end{aligned} \tag{10.64}$$

which has the solution

$$x = 1/(\nu+2), \quad y = -1/(\nu+2), \quad z = 2/(\nu+2). \tag{10.65}$$

Thus, we arrive at the dimensionally consistent equation

$$[R] = [E_0]^{1/(\nu+2)}[\rho_0]^{-1/(\nu+2)}[t]^{2/(\nu+2)}. \tag{10.66}$$

Hence, it follows that

$$R = S\left(\frac{E_0t^2}{\rho_0}\right)^{\frac{1}{(\nu+2)}} = \left(\frac{E_0t^2}{\alpha\rho_0}\right)^{\frac{1}{(\nu+2)}}, \tag{10.67}$$

where, for the spherically symmetric case, $\nu = 3$, and we arrive at eqn. (10.2). For $\gamma = 1.4$ and using *constant of proportionality* values for $\alpha$ and $S$ from Table 10.4, the problem

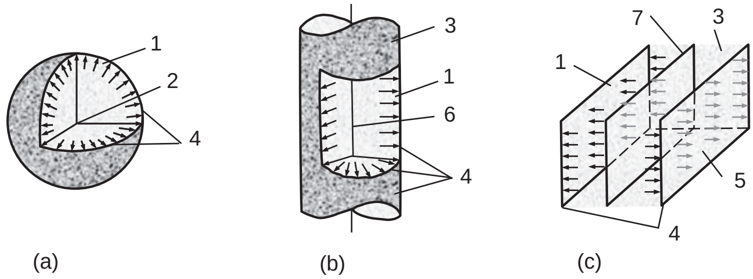


**Figure 10.11.** Blast waves in a compressible medium for (a) spherical, (b) cylindrical, and (c) planar geometry cases. Key: (1) moving medium, (2) symmetry center (of blast), (3) medium at rest, (4) shock wave front, (5) moving medium, (6) symmetry axis (of blast), (7) symmetry plane (of blast). Adapted from [Kor-91].

is fully defined.[4] The forms that a blast wave would take for the planar, cylindrical, and spherical cases are shown in Fig. 10.11.

For a point explosion in uniform ambient conditions, $E_0$ and $\rho_0$ are also constant. Therefore, for the spherically symmetric case, we have

$$R^5 t^{-2} = \text{constant}, \tag{10.68}$$

$$\Downarrow$$

$$\frac{5}{2}\log_{10}(R) - \log_{10}(t) = \text{constant}, \tag{10.69}$$

which is consistent with data from the time-lapsed photographs (see eqn. (10.40)). Also, on differentiating $R$ in eqn. (10.67) with respect to $t$, we obtain the velocity of the moving blast front, that is,

$$\frac{dR}{dt} = U = \frac{2}{5}\frac{R}{t}. \tag{10.70}$$

The downloads include code written for symbolic algebra programs Maple and Maxima (open source) that perform the preceding blast wave similarity analysis.

## 10.B APPENDIX: ANALYTICAL SOLUTION

Shortly after the numerical solutions published by Taylor, von Neuman, and Sedov, Sedov published a full analytical solution [Sed-59]. The analysis is rather lengthy, so we will just include some aspects that enable *point detonation* explosions in uniform ambient initial conditions to be tackled.

Using eqn. (10.67), which we repeat for convenience,

$$R = S\left(\frac{E_0}{\rho_0}t^2\right)^{\frac{1}{\nu+2}}, \tag{10.71}$$

[4] From Table 10.4 for $\gamma = 1.4$, we have the analytical value $\alpha_{sp} = E_0/E = 0.851$ for spherical geometry, $\alpha_{cyl} = 0.984$ for cylindrical geometry, and $\alpha_{pl} = 1.077$ for planar geometry. But $S = \alpha^{-1/(\nu+2)}$; therefore $S_{sp} = 1.0328$, $S_{cyl} = 1.0040$, and $S_{pl} = 0.9755$. See also [Feo-96] and [Kor-91, p74] for a discussion on approximations to $\alpha$.

https://doi.org/10.1017/CBO9781316336069.011 Published online by Cambridge University Press

the analytical solution can be derived from eqns. (10.1), the shock conditions

$$v_1 = \frac{2}{\gamma+1}u_s, \quad \rho_1 = \frac{\gamma+1}{\gamma-1}\rho_0, \quad p_1 = \frac{2}{\gamma+1}\rho_0 u_s^2, \quad u_s = \frac{2}{\nu+2}\frac{r_1}{t}, \tag{10.72}$$

where subscripts 0 and 1 refer to undisturbed ambient conditions and conditions immediately behind the shock wave respectively, together with the following set of relationships due to Sedov [Sed-59, p. 211, 217, 219]:

$$\begin{aligned}
\frac{r}{r_1} = \lambda = {}& \left[\frac{(\nu+2)(\gamma+1)}{4}V\right]^{-2/(2+\nu)} \left[\frac{\gamma+1}{\gamma-1}\left(\frac{(\nu+2)\gamma}{2}V - 1\right)\right]^{-\beta_2} \\
& \times \left[\frac{(\nu+2)(\gamma+1)}{(\nu+2)(\gamma+1) - 2[2+\nu(\gamma-1)]}\left(1 - \frac{2+\nu(\gamma-1)}{2}V\right)\right]^{-\beta_1}, \\
\frac{v}{v_1} = f = {}& \frac{(\nu+2)(\gamma+1)}{4}V\frac{r}{r_1}, \\
\frac{\rho}{\rho_1} = g = {}& \left[\frac{(\gamma+1)}{(\gamma-1)}\left(\frac{(\nu+2)\gamma}{2}V - 1\right)\right]^{\beta_3} \left[\frac{\gamma+1}{\gamma-1}\left(1 - \frac{\nu+2}{2}V\right)\right]^{-\beta_5} \\
& \times \left[\frac{(\nu+2)(\gamma+1)}{(\nu+2)(\gamma+1) - 2[2+\nu(\gamma-1)]}\left(1 - \frac{2+\nu(\gamma-1)}{2}V\right)\right]^{-\beta_4}, \\
\frac{p}{p_1} = h = {}& \left[\frac{(\nu+2)(\gamma+1)}{4}V\right]^{2\nu/(2+\nu)} \left[\frac{\gamma+1}{\gamma-1}\left(1 - \frac{(\nu+2)}{2}V\right)\right]^{\beta_5+1} \\
& \times \left[\frac{(\nu+2)(\gamma+1)}{(\nu+2)(\gamma+1) - 2[2+\nu(\gamma-1)]}\left(1 - \frac{2+\nu(\gamma-1)}{2}V\right)\right]^{\beta_4 - 2\beta_1}, \\
\frac{T}{T_1} = {}& \frac{p}{p_1}\frac{\rho_1}{\rho}, \; T_1 = \frac{p_1}{\mathcal{R}\rho_1},
\end{aligned} \tag{10.73}$$

where

$$\begin{aligned}
\beta_1 &= \frac{(\nu+2)\gamma}{2+\nu(\gamma-1)}\left[\frac{(2\nu(2-\gamma)}{\gamma(\nu+2)^2} - \beta_2\right], & \beta_2 &= \frac{1-\gamma}{2(\gamma-1)+\nu}, \\
\beta_3 &= \frac{\nu}{2(\gamma-1)+\nu}, & \beta_4 &= \frac{\beta_1(\nu+2)}{2-\gamma}, \\
\beta_5 &= \frac{2}{\gamma-1}, & \beta_6 &= \frac{\gamma}{2(\gamma-1)+\nu}, \\
\beta_7 &= \frac{[2+\nu(\gamma-1)]\beta_1}{\nu(2-\gamma)}.
\end{aligned} \tag{10.74}$$

$T$ represents temperature, $\mathcal{R}$ the ideal gas constant, and $u_s$ shock wave speed. Other symbols have been defined previously. Note that subscript 1 is used to indicate conditions immediately behind the shock, whereas in [Sed-59], the subscript 2 is used. Also, Sedov uses the symbol $\alpha_i$ for the indices in eqns. (10.73), rather than $\beta_i$.

With $\gamma > 1$ and $\nu \in (1, 2)$, values for $r = r_1\lambda, v = v_1 f, \rho = \rho_1 g$, and $p = p_1 h$ can be calculated by varying the nondimensional parametric variable $V$ in eqns. (10.73) and (10.74)

**Table 10.3.** Analytical data for the planar case $\nu = 1$ and $\gamma = 1.4$. Note the variable $f$ used by Sedov is not the same variable $f$ used by Tayor. Also, Sedov uses subscript 2 rather than 1 to indicate conditions appertaining immediately behind the shock wave position

| $\lambda = \frac{r}{r_1}$ | $\frac{r_0}{r_1}$ | $\frac{v}{v_1} = f$ | $\frac{\rho}{\rho_1} = g$ | $\frac{p}{p_1} = h$ | $f'$ | $g'$ | $h'$ |
|---|---|---|---|---|---|---|---|
| 1 | 1 | 1 | 1 | 1 | 1.5 | 7.5 | 4.5 |
| 0.9797 | 0.8873 | 0.9699 | 0.8625 | 0.9162 | 1.4688 | 6.1575 | 3.8131 |
| 0.9420 | 0.7151 | 0.9156 | 0.6659 | 0.7915 | 1.4067 | 4.3615 | 2.8352 |
| 0.9013 | 0.5722 | 0.8599 | 0.5160 | 0.6923 | 1.3367 | 3.1109 | 2.0959 |
| 0.8565 | 0.4501 | 0.8017 | 0.3982 | 0.6120 | 1.2597 | 2.2183 | 1.5250 |
| 0.8050 | 0.3427 | 0.7390 | 0.3019 | 0.5457 | 1.1758 | 1.5638 | 1.0723 |
| 0.7419 | 0.2448 | 0.6678 | 0.2200 | 0.4904 | 1.0802 | 1.0738 | 0.7067 |
| 0.7029 | 0.1980 | 0.6263 | 0.1823 | 0.4661 | 1.0390 | 0.8726 | 0.5483 |
| 0.6553 | 0.1514 | 0.5780 | 0.1453 | 0.4437 | 0.9921 | 0.6919 | 0.4022 |
| 0.5925 | 0.1040 | 0.5172 | 0.1074 | 0.4229 | 0.9438 | 0.5232 | 0.2648 |
| 0.5396 | 0.0741 | 0.4682 | 0.0826 | 0.4116 | 0.9144 | 0.4213 | 0.1838 |
| 0.4912 | 0.0529 | 0.4244 | 0.0641 | 0.4038 | 0.8947 | 0.3473 | 0.1289 |
| 0.4589 | 0.0415 | 0.3957 | 0.0536 | 0.4001 | 0.8849 | 0.3020 | 0.1003 |
| 0.4161 | 0.0293 | 0.3580 | 0.0415 | 0.3964 | 0.8750 | 0.2551 | 0.0453 |
| 0.3480 | 0.0156 | 0.2988 | 0.0263 | 0.3929 | 0.8651 | 0.1905 | 0.0237 |
| 0.2810 | 0.0074 | 0.2410 | 0.0153 | 0.3911 | 0.8602 | 0.1370 | 0.0111 |
| 0.2320 | 0.0038 | 0.1989 | 0.0095 | 0.3905 | 0.8584 | 0.1025 | 0.0089 |
| 0.1680 | 0.0012 | 0.1441 | 0.0042 | 0.3901 | 0.8574 | 0.0630 | 0.0029 |
| 0.1040 | 0.0002 | 0.0891 | 0.0013 | 0.3900 | 0.8572 | 0.0307 | 0.0005 |
| 0 | 0 | 0 | 0 | 0.3900 | 0.8571 | 0 | 0 |

subject to the constraints

$$\frac{2}{(\nu+2)\gamma} \leq V \leq \frac{4}{(\nu+2)(\gamma+1)}. \tag{10.75}$$

If $\nu = 3$ and $\gamma < 7$, then eqn. (10.75) also applies. For $\nu = 3$ and $\gamma > 7$, $V$ is subject to the following alternative constraints:

$$\frac{4}{5(\gamma+1)} \leq V \leq \frac{2}{5}. \tag{10.76}$$

Table 10.3 has been taken from [Sed-59] and contains solution data for $\nu = 1$ and $\gamma = 1.4$. It was generated using the preceding method and has been used in a numerical example included in Chapter 6.

Note that the Sedov variables $\lambda, f, g$, and $h$ correspond to the Taylor variables $\eta$, $\frac{\gamma+1}{2}\phi$, $\frac{\gamma-1}{\gamma+1}\psi$, and $\frac{\gamma+1}{2}f$, respectively (see eqns. (10.3), (10.29), (10.31), and (10.54)).

R code that can be used to generate similar tables to Table 10.3 for $\nu = 2, 3$ and plot the results is included in Listing 10.4.

## 10.B.1 Closed-Form Solution

If we neglect energy loss due to radiation and consider only very short periods following detonation, the total energy contained within the region from the point of detonation to the edge of the shock wave is constant throughout the period of blast expansion. It is equal to the sum of kinetic and internal energies, which can be expressed by the following integral:

$$E_0 = \mathrm{Co}\int_0^{r2} \left(\tfrac{1}{2}\rho v^2 + \rho e\right) r^{\nu-1} dr,$$
$$\mathrm{Co} = \begin{cases} 4\pi, & \nu = 3, : \text{spherical case}, \\ 2\pi, & \nu = 2, : \text{cylindrical case}, \\ 2, & \nu = 1, : \text{planar case}, \end{cases} \tag{10.77}$$

which, for the spherical case, is equivalent to eqns. (10.32) and (10.33) used by Taylor.

If we substitute $r = \lambda r_1, v = v_1 f, r = \lambda r_1$, and $\rho e = p/(\gamma - 1)$ into eqns. (10.77), then on using the shock conditions of eqns. (10.72), we arrive at

$$E_0 = \frac{8\,\mathrm{Co}\,\rho_1 {r_1}^{\nu+2}}{(\nu+2)^2(\gamma^2-1)t^2}\int_0^1 (gf^2 + h)\lambda^{\nu-1} d\lambda. \tag{10.78}$$

But from eqn. (10.67) we see that $\rho_1 r_1^{\nu+2}/t^2 = E_0/\alpha$. Therefore, on rearranging and splitting the integral into two parts, we obtain

$$J_1 = \int_{V_0}^{V_1} \frac{1}{2}\frac{\gamma+1}{\gamma-1} g V^2 \lambda^{\nu+1}\left(\frac{d\lambda}{dV}\right) dV,$$
$$J_2 = \int_{V_0}^{V_1} \frac{8h\lambda^{\nu-1}}{(\nu+2)^2(\gamma^2-1)}\left(\frac{d\lambda}{dV}\right) dV, \tag{10.79}$$
$$\alpha = \mathrm{Co}(J_1 + J_2),$$

where we have used the relationship $f = \frac{1}{4}(\nu+2)(\gamma+1)V\lambda$ from eqns. (10.73). We have also changed the integration variable from $\lambda$ to $V$, with a corresponding change in integration limits from eqn. (10.75). Also, the following expression for the analytical derivative of $\lambda$ with respect to $V$ is obtained from eqns. (10.73):

$$\frac{d\lambda}{dV} = -\frac{\lambda(8 + \gamma(\nu+2)^2(\gamma+1)V^2 - 4(\nu+2)(\gamma+1)V)}{(-2 + (2 + \nu\gamma - \nu)V)V(-2 + \gamma(\nu+2)V)(\nu+2)}. \tag{10.80}$$

Finally, for a given $\nu$ and $\gamma$, eqns. (10.79) can be integrated (numerically), using the relationships for $g, h$, and $\lambda$ from eqns. (10.73), to give a value for alpha. Thus, for known ambient gas conditions and geometry, the complete solution has been established.

The downloads include code written for symbolic algebra programs Maple and Maxima (open source) that derive the Sedov integrals of eqns. (10.79).

Some $\alpha$ and $S$ values for different cases are given in Table 10.4—recall from eqn. (10.67) that $S = \alpha^{-1/(\nu+2)}$.

The R code used to generate the values in Table 10.4 is included in Listing 10.4. It also generates Figs. 64–66 from [Sed-59] for given values of $\nu$ and $\gamma$. The code should be self-explanatory, but it is worth mentioning that the program uses the excellent function `quad()`, from the R package `pracma`, that performs the numerical integration of the two parts of the energy integral, $J_1$ and $J_2$. A theoretical discussion relating to the algorithm used in function `quad()` is given in [Gan-00].

**Table 10.4.** Values for constants $\alpha$ (used by Sedov) and $S$ (used by Taylor) calculated for planar, cylindrical, and spherical cases with $\gamma = 7/5$ and $\gamma = 5/3$

| | $\alpha$ | | S | |
|---|---|---|---|---|
| **Geometry** | $\gamma$=7/5 | $\gamma$=5/3 | $\gamma$=7/5 | $\gamma$=5/3 |
| Pl, $\nu = 1$ | 1.077 | 0.603 | 0.9755 | 1.1837 |
| Cyl, $\nu = 2$ | 0.984 | 0.564 | 1.0040 | 1.1538 |
| Sp, $\nu = 3$ | 0.851 | 0.494 | 1.0328 | 1.1517 |

```
# File: SedovCalc.R
require(compiler)
enableJIT(3)
rm(list = ls(all = TRUE)) # Delete workspace
library("pracma")

f <- function(V,gamma,nu){
  f <- (nu+2)*(gamma+1)/4 * V * lambda(V,gamma,nu)
}
g <- function(V,gamma,nu){
  g <- ((gamma+1)/(gamma-1)*
         ( (nu+2)*gamma/2 * V-1))^(beta[3]) *
    ((gamma+1)/(gamma-1)*(1-(nu+2)/2 * V))^(beta[5])*
    ((nu+2)*(gamma+1)/((nu+2)*(gamma+1)-2*(2+nu*(gamma-1)))*
       (1-(2+nu*(gamma-1))/2 *V ) )^(beta[4])
}
h <- function(V,gamma,nu){
  h <- ((nu+2)*(gamma+1)/4*V)^(2*nu/(2+nu)) *
    ((gamma+1)/(gamma-1)*(1-(nu+2)/2 * V))^(beta[5]+1)*
    ((nu+2)*(gamma+1)/((nu+2)*(gamma+1)-2*(2+nu*(gamma-1)))*
       (1-(2+nu*(gamma-1))/2 *V ) )^(beta[4]-2*beta[1])
}
lambda <- function(V,gamma,nu){
  lambda <- ((nu+2)*(gamma+1)*V/4)^(-2/(2+nu)) *
    ((gamma+1)/(gamma-1)*((nu+2)*(gamma/2)*V - 1))^(-beta[2])*
    ((nu+2)*(gamma+1)/((nu+2)*(gamma+1)-2*(2+nu*(gamma-1)))*
       (1-(2+nu*(gamma-1))*V/2))^(-beta[1])
}
dlambdadV <- function(V,gamma,nu){
  dlambdadV <- -lambda(V,gamma,nu)*(8+gamma*(nu+2)^2*(gamma+1)*V^2-
                  (4*(nu+2))*(gamma+1)*V)/
                  ((-2+(2+nu*gamma-nu)*V)*V*(-2+gamma*(nu+2)*V)*(nu+2)+eps)
}
betaSet <- function(gamma,nu){
  beta <- rep(0,7)
```

```
  beta[2] <- (1-gamma)/(2*(gamma-1)+nu)
  beta[1] <-(nu+2)*gamma/(2+nu*(gamma-1)) *
              ((2*nu*(2-gamma))/(gamma*(nu+2)^2) - beta[2])
  beta[3] <- nu/(2*(gamma-1)+nu)
  beta[4] <- beta[1]*(nu+2)/(2-gamma)
  beta[5] <- 2/(gamma-2)
return(beta)
}
dJ1 <- function(V){
  dJ1dV <- (gamma+1)/(2*(gamma-1))*lambda(V,gamma,nu)^(nu+1)*
           g(V,gamma,nu)*V^2*dlambdadV(V,gamma,nu)
  return(dJ1dV)
}
dJ2 <- function(V){
  dJ2dV <- 8/((gamma^2-1)*(nu+2)^2)*lambda(V,gamma,nu)^(nu-1)*
            h(V,gamma,nu)*dlambdadV(V,gamma,nu)
  return(dJ2dV)
}
aS <- function(V){
#     print(dJ1())
#     scan(quiet=TRUE)
  # Energy integral and beta calc - eqn. (54), Kamm (2007).
  J1 <- quad(dJ1, V0, V1, tol=10^-6)
  J2 <- quad(dJ2, V0, V1, tol=10^-6)
  #
  if(nu == 1){
    C0 <- 2
  }else{
    C0 <- 2*(nu-1)*pi
  }
  alpha <- C0 * (J1 + J2)
  S <- alpha^(-1/(nu+2))
  return(c(alpha,S))
}
# Eqns. (11.15) and (11.16) from Sedov (1959).
N <- 100
eps <- 1e-60
nu <- 3 # 1,2,3
gamma <- 7/5 # 5/3
V0 <- 2/((nu+2)*gamma)
V1 <- 4/((nu+2)*(gamma+1)) # eqn. (11.14a)
V <- seq(V0, V1, length.out=N)
beta <- betaSet(gamma,nu)
# Plot results for given nu and gamma - Sedov Figs (64,65,66)
plot(lambda(V,gamma,nu),f(V,gamma,nu),type="l",lwd=3,col="red",
     xlab=expression(paste(lambda)),ylab="f, g, h")
```

```
lines(lambda(V,gamma,nu),g(V,gamma,nu),lwd=3,col="blue")
lines(lambda(V,gamma,nu),h(V,gamma,nu),lwd=3,col="green")
legend("top",lwd=c(3),lty=1,bty="n",
       legend=c("f","g","h"),
       col=c("red","blue","green"))
grid(nx = NULL, ny = NULL, col="lightgray", lwd = 1, lty=1)
#
aSvec <- aS(V)
alpha <- aSvec[1]
S <- aSvec[2]
```

**Listing 10.4.** File: `SedovCalc.R`—Code of program that performs the Sedov analytical calculations of eqns. (10.73) and (10.74) and plots results

### 10.B.2 Additional Complexity

The problem considered previously with constant ambient conditions can be readily extended to situations where the blast takes place in an incompressible medium or in a gas with variable density. For discussion on these and other cases, the reader is referred to [Sed-59], [Kor-91], [Boo-94], [Kam-00], and [Kam-07].

### 10.B.3 The Los Alamos Primer

As additional background to the preceding analysis, it is interesting to read the technical briefing that new recruits were given as an introduction to the Manhattan Project. The briefing was given as a course of five lectures by American phyisicist Dr. Robert Serber as an *indoctrination course* during the first two weeks of April 1943. A set of classified notes, written up by nuclear physicist Edward U. Condon, was printed at Los Alamos under the title *The Los Alamos Primer*. It was declassified in 1963 and is now in the public domain and available online at https://commons.wikimedia.org/wiki/File:Los_Alamos_Primer.pdf. This document summarizes what was known regarding nuclear explosions around 1943. It was subsequently published as a book by the University of California Press [Ser-92].

At the end of World War II, Serber joined the faculty at Columbia University and later became professor and chair of its physics department.

## REFERENCES

[Bet-47] Bethe, H. A., K. Fuchs, J. O. Hirschfelder, J. L. Magee, R. E. Peierls J. von Neumann (1947), Blast Wave, *Los Alamos Scientific Laboratory Report LA-2000*.

[Boo-94] Book, D. L. (1994), The Sedov Self-Similar Point Blast Solutions in Nonuniform Media, *Shock Waves* **4**-1, 1–10. doi:10.1007/BF01414626.

[Deb-58] Deb Ray, G. (1958), An Exact Solution of a Spherical Blast Under Terrestrial Conditions, *Proc. Natn. Inst. Sci. India* A **24**, 106–112.

[Dtr-07] DTRA (2007), Operation Trinity, Public Affairs Fact Sheet, *Defense Threat Reduction Agency (DTRA)*, available online at http://www.dtra.mil/documents/ntpr/factsheets/Trinity.pdf.

[Feo-96] Feoktistov, L. P. (1996), Self-Similarity-Particular Solution or Asymptote?, *JETP* **83**, 996–999.

[Gan-00] Gander, W. and W. Gautschi (2000), Adaptive Quadrature-Revisited, *BIT Numerical Mathematics* **1**, 84–101.

[Kam-00] Kamm, J. R. (2000), Evaluation of the Sedov–von Neumann–Taylor Blast Wave Solution, *Los Alamos National Laboratory Report LA-UR-00-6055*.

[Kam-07] Kamm, J. R. and F. X. Timmes (2007), On Efficient Generation of Numerically Robust Sedov Solutions, *Los Alamos National Laboratory Report LA-UR-07-2849*.

[Kor-91] Korobeinikov, V. P. (1991), *Problems of Point-Blast Theory*, American Institute of Physics.

[Mac-49] Mack, J. E. (1947), Semi-popular motion picture record of the Trinity explosion, MDDC221, U.S. Atomic Energy Commission.

[Pet-08] Petruk, O. (2008). Approximations of the Self-Similar Solution for Blastwave in a Medium with Power-Law Density Variation, *arXiv Preprint Astro-ph/0002112v1*, 1–17, available online at http://arxiv.org/abs/astro-ph/0002112.

[Sed-46] Sedov, L. I. (1946), Propagation of Strong Shock Waves, *Journal of Applied Mathematics and Mechanics* **10**, 241–250.

[Sed-59] Sedov, L. I. (1959), *Similarity and Dimensional Methods in Mechanics*, Academic Press.

[Ser-92] Serber, R. (1992), *The Los Alamos Primer, the First Lectures on How to Build an Atomic Bomb*. Annotated by Robert Serber. Edited with an introduction by Richard Rhodes. University of California Press.

[Tay-41] Taylor, G. I. (1941), The Formation of a Blast Wave by a Very Intense Explosion, *British Civil Defence Research Committee*, Report RC-210.

[Tay-46] Taylor, G. I. (1946), The Air Wave Surrounding an Expanding Sphere, *Proceedings of the Royal Society of London, Series A* **186**, 273–292.

[Tay-50a] Taylor, G. I. (1950), The Formation of a Blast Wave by a Very Intense Explosion. I. Theoretical Discussion, *Proceedings of the Royal Society of London, Series A* **201**, 159–174.

[Tay-50b] Taylor, G. I. (1950), The Formation of a Blast Wave by a Very Intense Explosion. II. The Atomic Explosion of 1945, *Proceedings of the Royal Society of London, Series A* **201**, 175–186.